Chapter 3

Meteorological and chemical processes

Key points

- The concentration of NO_2 at a given location is determined by a combination of emissions, meteorology and chemistry.
- NO_2 may be dominated by primary sources (i.e. direct emission), secondary sources (i.e. chemical formation), or may have significant contributions from both. It is a vital issue for policy whether the origin of the NO_2 at a given location is primary or secondary, because source-receptor relationships are dramatically different for primary and secondary pollutants.
- Meteorological processes operating on scales from a few metres to hundreds of kilometres play an important role in controlling dispersion and accumulation of NO_2.
- Very low wind speeds, temperature inversions and a shallow stable boundary layer are necessary conditions for winter NO_2 episodes.
- Limited meteorological observations in complex environments, such as in urban areas, leads to questions over sampling representativeness and model parameterisations which are not fully tested.
- Model simulations of NO_2 concentrations are sensitive to inter-annual variations in meteorological conditions.
- The chemical coupling of NO_x with ozone (O_3) plays a central role in determining the ambient level of secondary NO_2. Because of this chemical coupling, it is often convenient to define NO_2 and O_3 collectively as oxidant (OX).
- Other chemical processes may lead to additional NO to NO_2 conversion under specific conditions such as urban episodes during stagnation events.
- Chemical transformations of NO_x can generate a variety of inorganic and organic oxidised nitrogen compounds. Of these, HONO and PAN potentially contribute to measurements of NO_2 made using chemiluminescent analysers with thermal converters. The level of interference is likely to be small under the majority of ambient conditions.

3.1. Introduction

269. The concentration of NO_2 at a given location is determined by a number of factors. These include the magnitude and proximity of NO_x emissions sources, the rate at which these emissions are dispersed and the area over which they are transported (i.e. meteorology of winds, turbulent mixing and dilution), and the processes which determine what proportion of NO_x is in the form of NO_2 (that is, in addition to the proportion of NO_x directly emitted as NO_2, the chemistry leading to subsequent generation and destruction of NO_2). Accordingly, models which attempt to describe the concentration distribution of NO_2 in air must ideally contain an adequate representation of emissions, meteorology and chemistry.

270. A detailed description of the sources of NO_x and how the emissions density varies spatially and temporally is provided in Chapter 2. The purpose of this chapter, therefore, is to provide a summary of current understanding of the fundamental meteorological and chemical processes that play a role in controlling the ambient level of NO_2. To put these processes into context, the

section concludes with a description of how emissions, dispersion and chemistry combine to determine the distribution of NO_2 in the vicinity of roads in rural and urban environments.

3.2. Meteorology and NO_2

3.2.1. Introduction

271. Variations in weather conditions on scales of metres to thousands of kilometres can all be shown to impact upon spatial and temporal variations in NO_2 concentration. For example:

- increases in hemispheric scale background O_3 concentration may, if transported down into the urban boundary and canopy layers, become available as additional oxidant in urban environments.
- the familiar weather patterns which appear on television and newspaper weather maps, with their associated wind fields and stability conditions, control the degree of accumulation of air pollutants and the advection of primary and secondary pollutants from upwind sources and provide a context for local meteorological variations.
- local wind circulations, such as land-sea breezes and urban-country breezes, help to maintain ventilation and minimise the accumulation of NO_2 and its precursors. Conversely urban areas may act to block and divert the larger scale flows, and within urban areas topographical features such as rivers and hills may channel and modify the local wind patterns.
- microscale local meteorological variations occur in heterogeneous environments such as towns and cities as a result of roughness variability, varying degree of shade, anthropogenic energy sources, and modified moisture budgets. Vehicle movements also initiate localised turbulence which can be important in the local dispersion process.

272. The importance of all these meteorological scales are highlighted in this chapter, with an emphasis on their relevance to air pollution modelling and to the meteorological conditions which have accompanied important observed NO_2 episodes in the UK over the last decade. The section ends with some commentary on relevant meteorological trends over recent decades together with projections over the next century which have been simulated using climate models.

3.2.2. The atmospheric boundary layer

273. Pollutants emitted into the atmosphere are generally transported, dispersed and deposited in the lowest part of the atmosphere – the atmospheric boundary layer. A description of the airflow and turbulent motions within this layer is therefore helpful in understanding the dispersion of pollutants and this forms the subject matter of this section. Factors affecting the boundary layer structure and common features of the boundary layer over flat terrain are briefly described. There then follows a section on dispersion over flat terrain before a discussion of meteorology and dispersion in more complex situations such as the urban environment.

3.2.2.1 Factors determining boundary layer structure

274. The mean flow, turbulence and the temperature distribution in the atmospheric boundary layer are broadly governed by three groups of factors which are as follows:

- Heating at the surface which generates convective turbulence. This is determined by such factors as the solar radiation reaching the surface and the absorption and release of latent heat by water vapour. Urban surfaces and buildings modify the absorption and reflection of solar radiation and sensible heat fluxes. They also enhance run-off following rain, and affect evaporation.
- The roughness and changes in elevation of the earth's surface near and for some distance upwind of the region of interest.
- The roughness effect is caused by surface obstacles or roughness elements obstructing and hence decelerating the airflow; these may range in scale from grass to buildings and even ranges of hills. A 'roughness length' can be used to characterise the effect of these elements on the flow above them with large elements generally causing more deceleration and greater turbulence levels and hence greater mixing of pollution. Within the obstacles, as occurs in an urban area, the flow is more complex as discussed in Section 3.2.3.
- The effects of changes in elevation on the airflow are characterised both by the heights and the length scales of the terrain features and may be very complex. Typically the flow accelerates over hill summits and decelerates up and downwind. As the hill slopes increase there can be regions of separation (downstream) and blocking (upstream) with the flow direction reversing, resulting in very complex dispersion of pollution. Local solar heating effects or cooling effects can result in anabatic (upslope) and katabatic (downslope) winds, or local circulations over water or park areas.
- Finally the airflow at the top boundary layer determined by the large scale pressure gradient broadly determines wind speeds. However in light or calm winds the airflow patterns are strongly affected by local heating effects for example from buildings and by local features such as slopes or valleys.

3.2.2.2 Typical boundary layer structure over flat terrain

275. Within the atmospheric boundary layer there are three broad types of structure corresponding to (i) unstable/convective boundary layers, (ii) neutral boundary layers and (iii) stable boundary layers. Typical conditions characterising these structures are for (i) light winds, and strong surface heating and consequently strong vertical mixing; for (ii) high winds and/or weak surface heating or cooling; and for (iii) night time conditions of light winds and negative surface heat flux (cooling) respectively.

276. In the neutral boundary layer the mean flow and turbulence are determined by the drag of the flow over the surface. The increase of mean flow U with height z can be described by a simple logarithmic formulation as

$$U(z) = \frac{u_*}{\kappa} \ln\left(\frac{z}{z_0}\right)$$

where u_* is the friction velocity related to the surface shear stress and turbulence levels and z_0 a representative surface roughness typically a few centimetres in rural areas and over 1 m in the most built up urban centres. (κ is von Karman's constant (0.4)).

277. In built up areas the flow above the buildings reacts as if the surface is significantly higher than z_0, typically over 50% of the building height. This effective height is often referred to as the zero plane displacement.

278. Both lengthscales and timescales of turbulence are important in determining the rate of spread or mixing of a dispersion plume and the chemical reaction rates. For instance chemical reaction rates are limited by turbulent mixing rates if the turbulent mixing timescale is greater than chemical reaction timescales (i.e. the reaction can proceed only after the reactive species have been mixed together). In a neutral boundary layer over flat terrain this timescale is approximately 0.3 z/u_*, ranging from a few to hundreds of seconds; in the urban canopy the timescale can be determined by building height (h_B) and is roughly h_B/u_* (tens of seconds).

279. In the convective boundary layer the surface heat flux F_{ϑ_0} provides an additional input of turbulent energy and the vertical component of turbulence can increase with height which is very important in the dispersion of elevated sources of pollutant. A useful parameter is the Monin Obukhov length, L_{MO}, which is a length scale used to denote the relative importance on turbulence generation of surface drag and surface heating

$$L_{MO} = \frac{-u_*^3}{\kappa g F_{\theta 0} / \left(\rho c_\rho T_0\right)}$$

where g, h, ρ, c_p and T_0 are the acceleration due to gravity, boundary layer height, density of air, specific heat of air and temperature respectively.

280. In convective conditions the L_{MO} is negative (implying an unstable layer) and decreases with increasing heat flux being a few tens of metres for strongly convective conditions. For a given L_{MO}, scales larger than $|L_{MO}|$ are dominated by convectively produced turbulence.

281. In the stable boundary layer surface cooling stably stratifies the surface layer which in turn inhibits the production of turbulence. Turbulence levels, lengthscales and mixing are smaller than those occurring in the neutral boundary layer and consequently the boundary layer height h is smaller. In stable layers the Monin Obukhov length (L_{MO}) corresponds approximately to the largest turbulent length scales with scales decreasing as the cooling increases and hence L_{MO} decreases.

282. Over urban areas the general description of the idealised atmospheric boundary layer structure given above only applies to the flow above the urban canopy with the bulk impact of the urban canopy represented by a higher surface roughness (for example, z_0 = 1m) and with allowance made for anthropogenic inputs to the heat flux. Some discussion of effects within the urban canopy appears in Section 3.2.3.

3.2.2.3 Dispersion over flat terrain

283. In Figures 3.1.1 and 3.1.2 a dispersion model based on many of the principles described in this chapter, ADMS 3 (Carruthers *et al*., 1994), has been used to illustrate how in general terms the ground level concentration (glc) of a pollutant emitted from a point source varies with distance downwind from the source over flat terrain. Figure 3.1.1 is for a ground level source whilst Figure 3.1.2 is for an elevated source. The concentration is for an averaging time of one hour which is generally smaller than the timescale of typical changes in meteorology, but larger than the timescales of turbulence fluctuations in concentration. The weather conditions range from Case 1 (very unstable), through to Case 2 (neutral), through to Case 3 (very stable).

284. For the ground level source the maximum surface concentration occurs at the release point and then decays away from the source with the rate of decay being highest for the most unstable conditions, because of rapid turbulent mixing, and lowest for the most stable case, because of very weak turbulence. Thus ground level concentrations remain quite high well downwind of sources in stable conditions.

285. For the elevated source, Figure 3.2, the position of maximum surface concentration is downstream of the source since the pollutant has to be mixed down to the surface. The highest surface concentrations occur in the most unstable conditions because of rapid vertical mixing and also because the skewed nature of the vertical component of turbulence brings the plume centreline down towards the surface. This also results in the position of the surface maximum being closest to the source for unstable conditions. As conditions become less convective and finally stable the maximum surface concentration decreases whilst the downwind distance of greater impact at ground level increases significantly.

Figure 3.1 Variations of ground level concentration (µg m^{-3}) with downwind distance for a ground level point source. Emission rate 0.01 g s^{-1}, wind speeds for unstable, neutral and stable flow are 2, 4 and 2 ms^{-1} respectively.

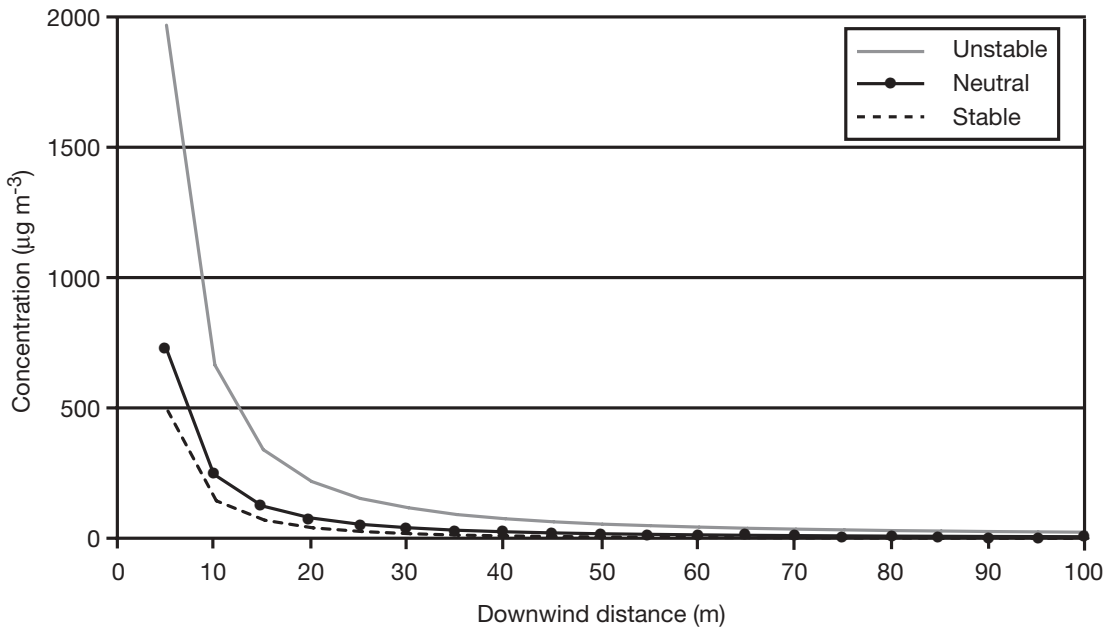

Figure 3.2 Variation of ground level concentration with distance for an elevated point source of height 99 m. The emission rate is 2 g s^{-1}. Wind speeds are as for Figure 3.1.

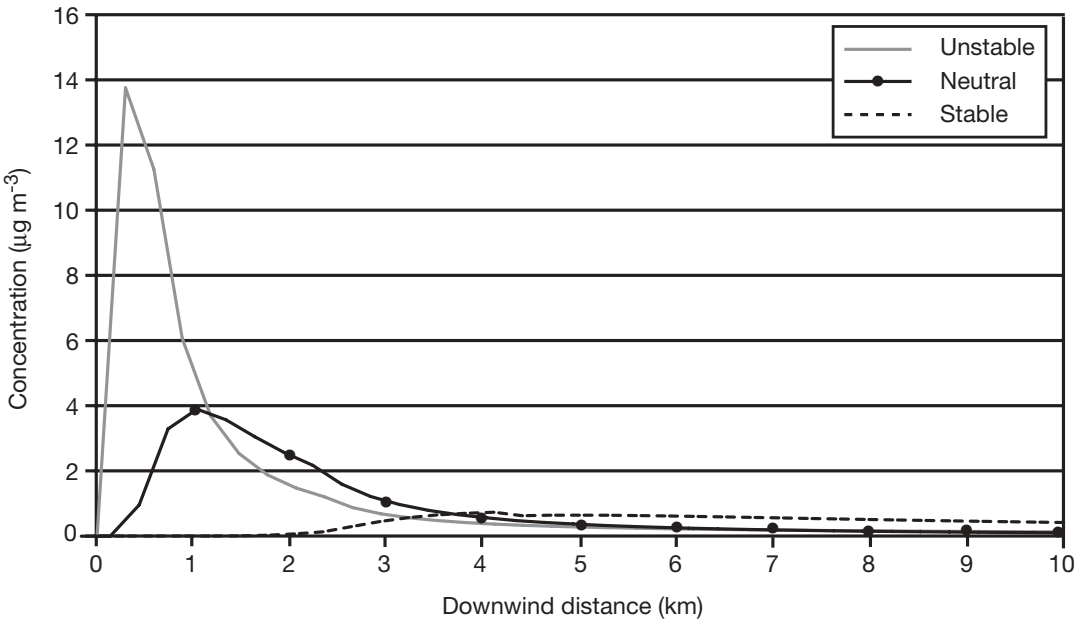

3.2.3. Urban meteorology

286. Exceedences of NO_2 objective limits are likely to be associated with urban areas, caused primarily by the NO_x emissions within urban areas. Winter episodes of very high concentrations of primary pollution, such as NO_x in urban areas, are associated with a high temperature-wind index according to Middleton and Dixon (2001), but secondary episodes of NO_2, for example, are more dependent on regional meteorology.

287. A purely deterministic description of the levels of NO_2 within an urban area would require a full description of emissions, dispersion and chemistry over very short spatial and temporal scales, which current models do not treat explicitly. Instead existing NO_2 models are either semi-empirical relying on a large set of relevant data, or attempt to describe these complex processes in an idealised way. The strong dependence of NO_2 on oxidant which tends to have a smoother, regional distribution, attenuates local concentration gradients. The calculation of primary pollution concentrations, such as NO_x, depends much more strongly on factors associated with dispersion. NO_2 tends to be a small fraction of NO_x determined by oxidant levels except when NO_x concentrations are low. Therefore the sensitivity of NO_2 concentrations to uncertainty in the NO_2-NO_x relationship is more important than the large uncertainties in urban meteorological factors. In this report a number of such relationships are used but none appear to depend strongly on urban meteorological factors.

288. It is therefore unclear how exceedences of the long-term NO_2 objective depend on urban meteorological factors. However since many measurement sites are within urban areas, it is important to review qualitatively the factors in an urban area which could influence dispersion. Differences between wind measurements made at a meteorological site within and outside a city illustrate climatological differences between urban and rural areas, but do provide explicit information about the local, site-specific factors which influence urban dispersion. These factors are reviewed below, in which the dynamical and thermal effects of urban areas are discussed separately.

3.2.3.1 Urban dynamical and thermal effects

289. In contrast to rural areas, the urban boundary layer is more complex, as a roughness sublayer of much larger vertical extension than found in typical rural areas occupies the first tens of metres above the surface, with the remainder of the surface layer (the inertial sublayer) above. The roughness sublayer includes the urban canopy layer, which is composed of individual street canyons and other roughness elements (see Figure 3.3). This figure illustrates the widely varying scales of motion affecting urban pollution concentrations. These motions and the turbulence associated with them determine the rate of mixing of pollution within an urban area. Pollution measurements are made between buildings, whose presence on aggregate change wind profiles and structure in an urban area compared with surrounding rural areas. Several simplifying approaches to describing urban wind and turbulence profiles have been proposed recently, such as Rotach (2002), Martilli *et al.* (2002) and Soulhac *et al.* (2002). Figure 3.4 illustrates schematically complex dispersion produced by the re-circulating flow within a street canyon.

290. The WMO-guideline for rural stations considers wind measurements to be representative if placed 10 m above ground without close obstacles; temperature and humidity measurements should be conducted at 2 m. For urban areas, no WMO guidelines for proper siting exist (Oke, 1999). Only in the upper part of or above the surface layer are contributions from individual surface roughness elements blended into possible representative averages.

Figure 3.3 Schematic description of the urban boundary layer including its vertical layers and scales. (Oke, 1999).

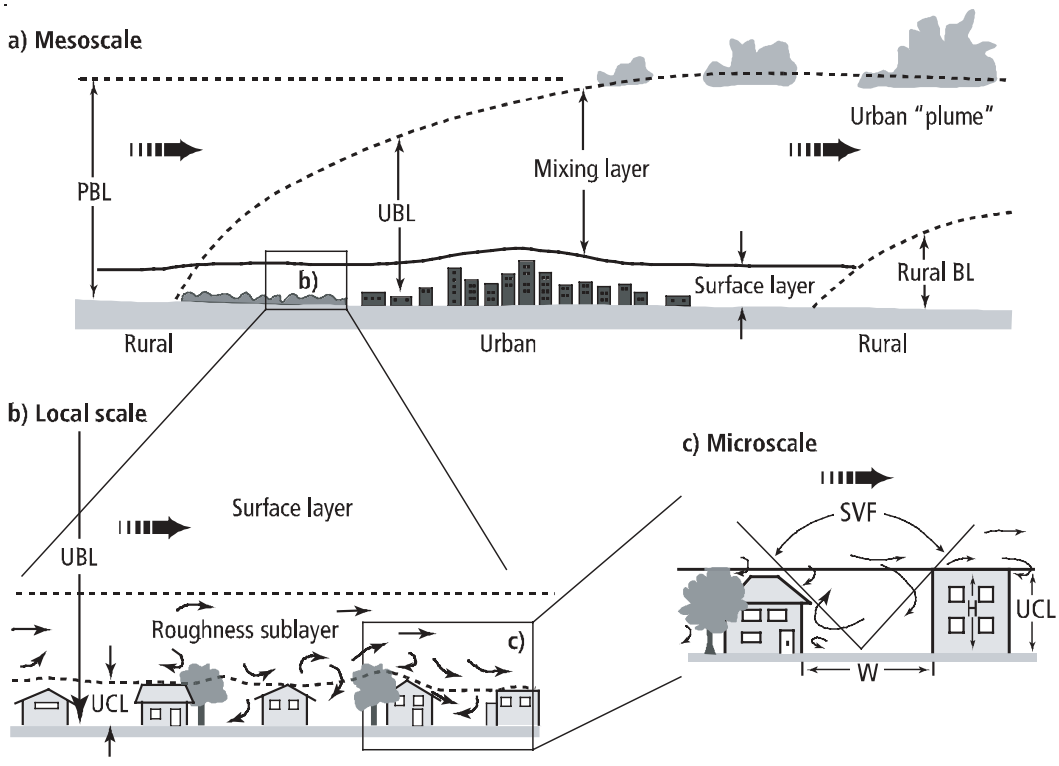

Figure 3.4 Schematic representation of the air flow within a street canyon.

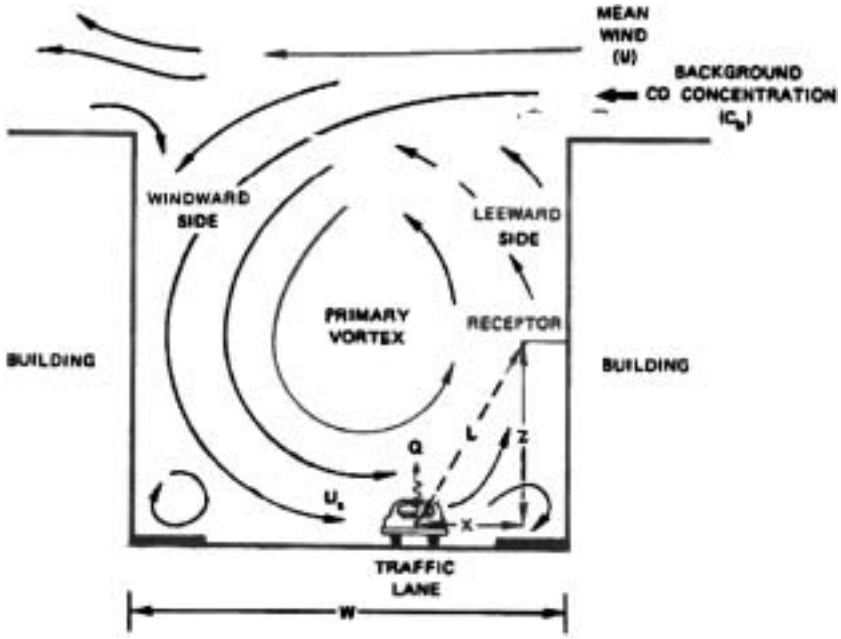

291. The heating of air near the surface of urban areas is an important factor determining dispersion in lower layers of the urban atmosphere and is determined by the energy balance. This is the key component of any model aiming to simulate the partitioning of dynamical and thermodynamical patterns (Piringer, 2001) between net radiation, the turbulent sensible and latent heat fluxes, respectively, the storage heat flux and additional sources of energy due to human activities.

292. In urban areas there are marked differences in energy partitioning compared to rural conditions, where most measurements have been performed. Knowledge of surface heat fluxes as well as atmospheric stability and surface roughness is essential for air pollution dispersion models. Normally the components of the surface energy balance, or its components, are not directly measured at meteorological stations. In the last decade, a series of local-scale energy balance observations have been conducted to test practical schemes for estimating surface heat fluxes. Middleton (2002) gives extra detail on the experimental studies currently under way within Europe. Assessing methods of determining the height of the urban boundary layer, which is dependent on the surface heat fluxes, is another important task.

293. Schemes have been developed to estimate net radiation, sensible heat flux and other urban boundary layer parameters from hourly standard meteorological data. Such meteorological pre-processing models are needed to calculate dispersion parameters related to meteorology, before a dispersion modelling calculation can be performed. The goal of recent research is an urban pre-processor scheme, which makes use of parameterisations that require standard meteorological observations, supplemented by basic knowledge of the surface character of the target urban area. One such scheme, LUMPS, has been shown to perform well when evaluated using data from North American cities (Grimmond and Oke, 2001). However, a review (Schatzmann *et al.*, 2001) of current methods of obtaining urban meteorological data in Europe for dispersion calculations concluded that many of the operational approaches to the pre-processing of meteorological data in urban areas have little justification.

3.2.3.2 Reduction in complexity

294. The basic premise of the meteorological pre-processing schemes is that heat fluxes can be modelled using net radiation, simple information on surface cover (area of vegetation, buildings and impervious materials), surface geometry (surface element roughness and density) and standard weather observations (air temperature, humidity, wind speed and pressure). The aim of these methods is to reduce the complexity in the description of the urban surface heat flux with a minimum increase in uncertainty

295. Of course there are situations where these methods do not apply. Since the methods are based on a one-dimensional energy balance, it is unlikely to perform well in areas where there is significant spatial variability in land cover or surface geometry, for example, at the urban-rural interface.

296. Simplification methods have also been applied to the aerodynamic properties of urban areas. The roughness length and zero plane displacement are the two main properties influencing the flow. Two broad methods have been proposed: the geometric method which uses parameters which broadly describe the geometric form, or micrometeorological methods that use observations of wind and turbulence to derive parameters from the logarithmic wind profile. The later method requires tall instrumented towers. Sodar and meteorological masts have been used to derive the roughness length and displacement length for Lille (Wrobleski *et al.*, 2001). The former method requires knowledge of certain average geometric factors describing urban roughness elements, such as the average height of roughness elements (buildings or trees), fractional plan area, fractional frontal area etc. Relationships can be derived from idealised flows over simplified arrays in wind tunnels, but need to be tested in real situations (Grimmond and Oke, 1999). A classification of effective terrain roughness is often valuable in working situations (Davenport *et al.*, 2000).

297. For an air quality calculation one needs to derive a number of dispersion parameters from the meteorological factors, such as roughness length, zero plane displacement, surface heat flux, boundary layer height. Some may be derived from routine urban measurements and some from formulae based on idealised conditions (usually by applying some scaling rule). There are other parameters which are related to dispersion rather than to local meteorology, such as the velocity in the street (or equivalently within the urban canopy u_C), the exchange velocity w_E between the street and the flow above, and the canopy length Lc equal to the distance required for the flow to adjust to the step change between the urban and rural roughness. Study of methods for deriving these parameters is still a matter of research (Hanna *et al.*, 2002).

298. u_C, w_E and Lc are parameters which should be specified if assessments of pollutant concentrations in and near streets are to be made. They are required input parameters if well-known models, such as CALINE4 for roadside concentrations, and OSPM for street canyon concentrations (street canyon models are reviewed by Vardoulakis *et al.,* 2002a) are to be applied. Such models are necessary if roadside concentrations are to be estimated.

299. Vardoulakis *et al.* (2003) have shown that the prediction of concentrations in street canyons is subject to considerable uncertainty, arising from various causes (such as the uncertainties in emissions, local meteorology and the description of processes within a model). Vardoulakis *et al.* (2002b) recommend an approach based on a mixture of measurements and models. The semi-empirical approaches used in this report to assess roadside concentrations avoid these difficulties. However, uncertainties then remain as to what is meant by a roadside concentration, and how the exposure to high concentrations (Vardoulakis *et al.,* 2002a) depends on local factors, such as street geometry, distance from road etc. For example the site in London Bloomsbury is under trees within a square, so that mixing of nearby traffic

emissions within the square will be different between summer and winter. The London Senator House site is located on the roof of an office block.

300. The London Marylebone Road site is within a street canyon, but the street does not consist of buildings of uniform height, nor are these continuous without gaps between them. Concentration gradients near to traffic emissions are steep, so that the estimated concentration along a road link, based on the aggregation of measurements made at various distances and locations near to different roads, represents an average which is difficult to define rigorously. One of the consequences of NO_x chemistry is that variations between different locations are likely to be attenuated reducing the seriousness of the problem. However, this is just one example of the difficulty of assessing what measurements at a site in an urban area represent.

3.2.3.3 Blending height

301. The problem of deciding what measurements at a single point within a region of spatially varying surface characteristics means, applies to both meteorological and pollution measurements. Applying a blending height, taken approximately to be 2.5 times the height of buildings, is a useful simplification. Above the blending height, effectively constant turbulence levels (described by the friction velocity) and roughness lengths can be defined for surfaces with inhomogeneous surface characteristics (spatially varying roughnesses or surface heat fluxes). Associated with the blending height are aggregation formulae, or weighted averages, of the surface characteristics. For the regional heat flux, a simple weighted average over the sub-areas of patches with different characteristics is used (Gryning and Batchvarova, 2001). For the effective roughness length a more complex averaging is needed. Such methods need to be tested, but are clearly essential for meso-scale models in which surface characteristics are averaged over some grid square, within which some effective exchange of heat or momentum is visualised to take place.

302. Meso-scale models are the main tool by which episodes of high pollution in urban areas are predicted, as shown by a review of European approaches conducted by Kukkonen (2001). In meso-scale models with scale of order 1 km, the main urban modification is to increase the roughness using a roughness length of order 1 m. This is defined by taking a logarithmic wind profile measured in the inertial sublayer, above the roughness sublayer. In an urban area the building density changes, and the urban boundary layer evolves and it is not obvious that a local roughness length can be defined. As described above pollution transport within the roughness sublayer is a further complication, but needs to be described in order to assess human exposure.

303. The so-called ‘urbanisation’ of meso-scale models is an important issue for improving urban pollution forecasts. Present methods include numerical weather prediction models, which may not see the urban area because the smallest horizontal length scale is too large. Finer scale models may have urban adjusted surface boundary conditions, or may have detailed descriptions of the urban neighbourhood nested within them (Baklanov *et al.*, 2002).

3.2.3.4 Inclusion of meteorology in urban dispersion calculations

304. The urban boundary layer height is the height to which the urban pollution mixes. Persistent low boundary layer heights are associated with pollution episodes as dilution is restricted. The blended surface heat flux is the appropriate quantity to use in estimating the height of the urban boundary layer (Baklanov, 2002). The literature is full of formulae (for example, Baklanov (2001)) for mixing height under stable conditions.

305. There are other features of urban areas for which there are at present no suggested practical formulae, for example on the relationship between the wind speed at a standard 10 m height outside a city to the wind speed on a mast, or above roof level within the city. Experimental results have been reported, for example:

- Roof-top wind (Leek U.K.) = 0.63 (airport wind at 10 m);
- Urban wind at 32 m (Lisbon) = 0.65 (rural wind at 10 m) + 1.24;
- Urban wind at 30 m (Copenhagen) = 0.51 (airport wind at 10 m);
- Urban wind at 30 m (Birmingham) = rural wind at 10 m.

306. Bezpalcova *et al.* (2002) have used numerical simulations to assess deviations from idealised wind profiles for simple cases of the urban atmospheric boundary layer. Thus the interpretation of the differences between measurements at Heathrow and the London Weather Centre is difficult.

307. Methods developed to describe dynamic and thermodynamic aspects of urban meteorology have application in the practical methods for predicting urban pollution levels based on source-receptor relationships. However within the roughness layer of the urban atmosphere which contains all the measurement sites, it is difficult to make recommendations. Belcher and Coceal (2002) introduce an additional spatial averaging term into the momentum equations describing the flow within the lower layers of the urban atmosphere. Similarly Carissimo and Macdonald (2001) introduce effective drag, and turbulence terms to describe the averaged flow equations within the urban canopy.

308. Even in situations when very detailed turbulence measurements are available above the roof canopy, for example, Basel, Hannover (Mueller *et al.*, 2002) and Nantes (Mestayer *et al.*, 2002) there is a need to extrapolate to other locations or positions. Pascheke *et al.* (2002) argue that the use of systematic wind tunnel experiments is the way to close gaps in field data. It is essential to identify urban meteorological issues relating to urban pollution assessments. In addition for practical use, advice needs to be given on urban correction factors. The starting point for this has been the inventory of urban meteorological stations, which now comprises over 300 sites from all countries active in COST 715 (Mueller *et al.*, 2002).

309. However the influence of meteorology is indirect. It is only one of many factors, which can influence urban pollution predictions. The outcomes of a pollution assessment are predictions of ground-level concentrations and the success of an assessment is judged against measurements of concentrations, not meteorological variables. Rotach (2001) has, for example, carried out this process using two urban simulations, one with and one without the roughness sublayer (as would normally be adopted in a dispersion calculation assuming surface characteristics prevail down to the ground). For limited measured data sets, the urban parameterisation performs better. A similar approach has been used to produce an urban meteorological pre-processor for Helsinki (Karppinen *et al.*, 2000), dividing the surface layer into an inertial and roughness sublayer and adopting an upper bound on surface cooling in stable atmospheric conditions, again showing differences in dispersion. These approaches have been applied to whole cities, namely Zürich (de Haan *et al.*, 2001) and Helsinki (Karppinen *et al.*, 2000). In the U.K. the application of ADMS Urban is a comparable approach.

3.2.3.5 Role of urban meteorology in NO_2 assessments

311. Urban meteorology is of major importance in assessing concentrations of primary pollutants, such as NO_x. A set of empirical curves may be used to represent the relationship between NO_2 and NO_x. The curves vary according to the type of source and the amount of oxidant available.

311. Thus the semi-empirical approaches to urban NO_2 concentration assessments provide an assessment method without the need to include urban meteorology explicitly. Given the current difficulties of describing urban meteorology this has some advantages. However the empirical approaches have the limitation that impact of certain factors cannot be evaluated. Therefore process models such as ADMS Urban, have been applied widely, with the more complex aspects of urban meteorology neglected They provide reasonably adequate assessments within a reasonable degree of uncertainty. Future work should be directed to including the more detailed influences of urban meteorology.

3.2.4. Station meteorological data for use in air pollution modelling

312. Since exposure to NO_2 is almost exclusively an urban problem in the UK, much attention is paid to the availability and quality of meteorological data from urban meteorological stations for use as input to modelling studies. Unfortunately:

- there are a declining number of urban weather stations as a result of recent changes to the monitoring network;
- it is difficult to collect meteorological data which sufficiently characterises the important range of environments which is typical of urban regions (Oke, 1999) and compromises in instrument exposure commonly have to be made;
- insufficient studies have been carried out comparing those urban measurements which do exist against upwind and downwind rural stations.

313. As a result there is a very incomplete understanding of the sensitivity of model results to the weather station selected as being most representative and to the particular year of data used. Rotach *et al*. (2001) are addressing this issue by designing monitoring strategies which consider the variation in meteorological conditions across a city both in the horizontal and the vertical plane.

314. The selection of meteorological data to be used as input to air pollution models is a crucial step and the following section highlights spatial and temporal issues which should be considered.

3.2.4.1 Variations between neighbouring stations

315. Table 3.1 and Figure 3.5 illustrate the difference between meteorological data recorded at Heathrow, London Weather Centre (LWC) and Marylebone Road. Note the lower wind speed at Heathrow and that the prevailing direction is backed relative to LWC. The LWC site is two metres above a 29 m building in Central London. The wind speed is retarded by the high roughness of Central London, but is greater than Heathrow because of the height of observation and flow speed-up over building top. The wind speeds measured in the Marylebone Road canyon can be seen to be significantly lower than at the other two sites.

Table 3.1 Summary of 1999 meteorological data.

	Heathrow			London Weather Centre		
Location and type	(507700, 176700) in the Heathrow airport/flat terrace			(530200, 180000) 2 m above building; Central London		
Height above ground	10 m			31 m		
Roughness length	0.2 m			1 m		
Data Capture	99.8%			95.9%		
Statistics	Mean	Minimum	Maximum	Mean	Minimum	Maximum
Temperature (°C)	11.8	-4.6	32.7	12.5	-1.3	31.9
Wind speed (m s^{-1})	3.1	0.0	12.9	4.0	0.5	12.9
Cloud cover (oktas)	5.6	0.0	8.0	5.5	0.0	8.0

Figure 3.5 Windroses for meteorological data from London for 1999.

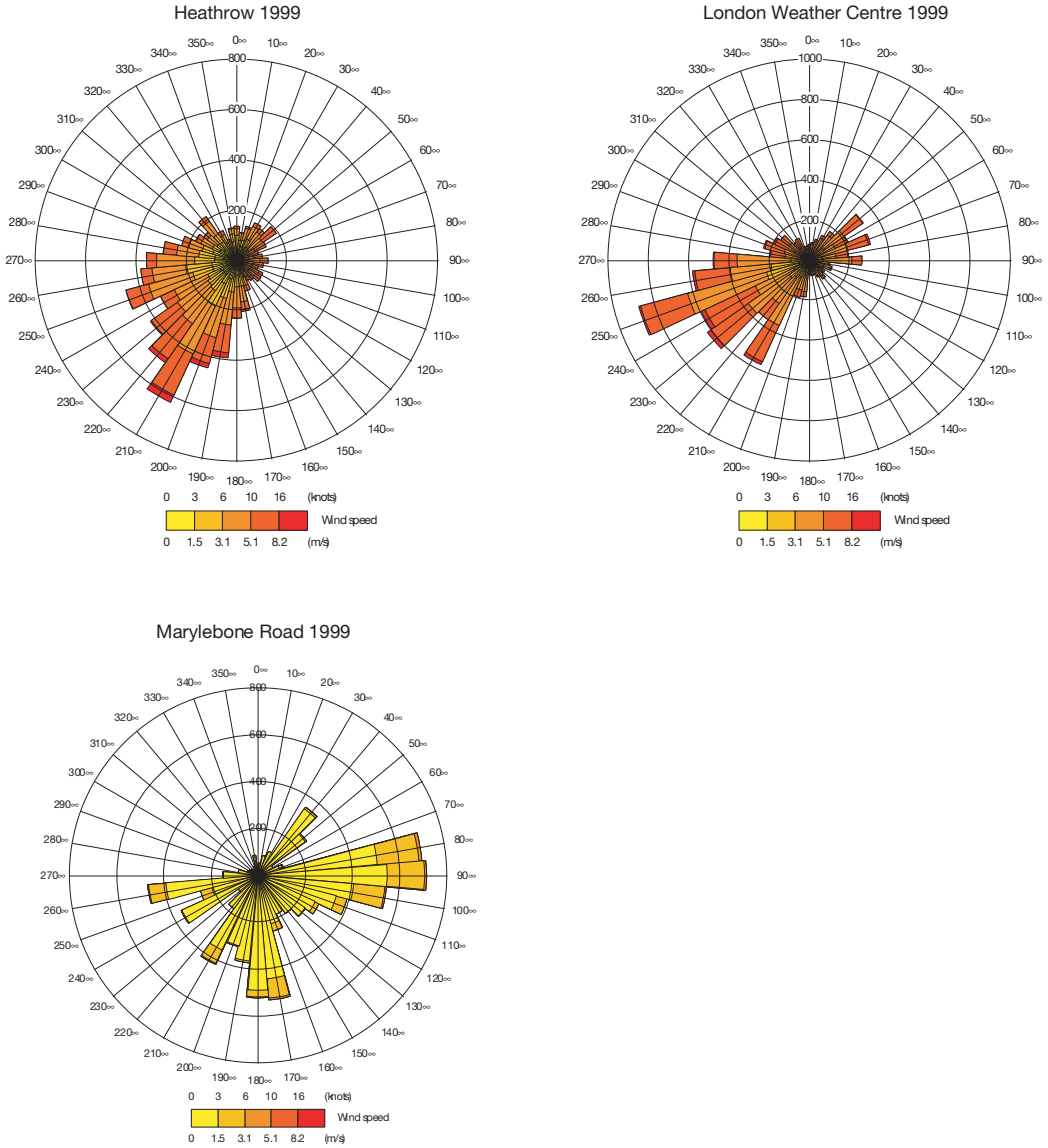

3.2.4.2 Inter-annual variations

316. Inter-annual variations in meteorology are thought to impact annual average concentrations by no more than ±15% (Defra, 2003). Middleton and Dixon (2001) show how significant inter-annual differences in wind roses and frequency of 'calm' conditions can be observed at a single monitoring station (Heathrow Airport). Sensitivity studies are recommended which take account of this potential, including 'worst case' scenarios.

3.2.5. NO_2 episodes

3.2.5.1 Classification methods

317. A number of tools have been and continue to be used in analysis of weather conditions accompanying poor air quality conditions:

- Station wind roses (for example, Middleton and Dixon, 2001)
- Isobaric, geopotential height and windfield analyses from numerical weather prediction models (for example, Dorling and Doyle, 2003)
- Back trajectories (for example, Stohl, 1998; Jenkin *et al.*, 2002)
- Subjective and Objective Weather Type Classifications (for example, Davies *et al.*, 1991; Buchanan *et al.*, 2002)
- Stagnation Indices (for example, Middleton and Dixon, 2001; Wang and Angell, 1999; Dorling *et al.*, 2003)

318. In many cases a number of these are used in combination in order to add further confidence to the interpretation.

319. Wintertime NO_2 episodes are strongly related to the incidence of periods of air stagnation and the accumulation of pollution from local sources. Summertime episodes, meanwhile, are affected by the advection of O_3 from upwind sources. Since the frequency of these important episode-related weather conditions varies from year to year, trends in precursor emissions can be masked by inter-annual variations in meteorology.

320. Dorling and Doyle (2003) have attempted to capture the variability in seasonal synoptic scale weather patterns by clustering daily fields of the height of the 850 hPa pressure surface , over the period 1991-2001, using the NCEP re-analysis dataset (Kalnay *et al*., 1996). Such an approach is arguably best suited to reviewing variation in weather conditions over an extended period. The dataset is divided into 5-day non-overlapping periods and ten clusters are retained in each season (DJF, MAM, JJA, SON). As examples, Figures 3.6 and 3.7 show the geographical domain considered and the middle day of each cluster for winter and for summer.

Figure 3.6 Winter 850 hPa pressure surface height (metres) clusters (cluster 1 top left, cluster 2 bottom left, cluster 10 bottom right).

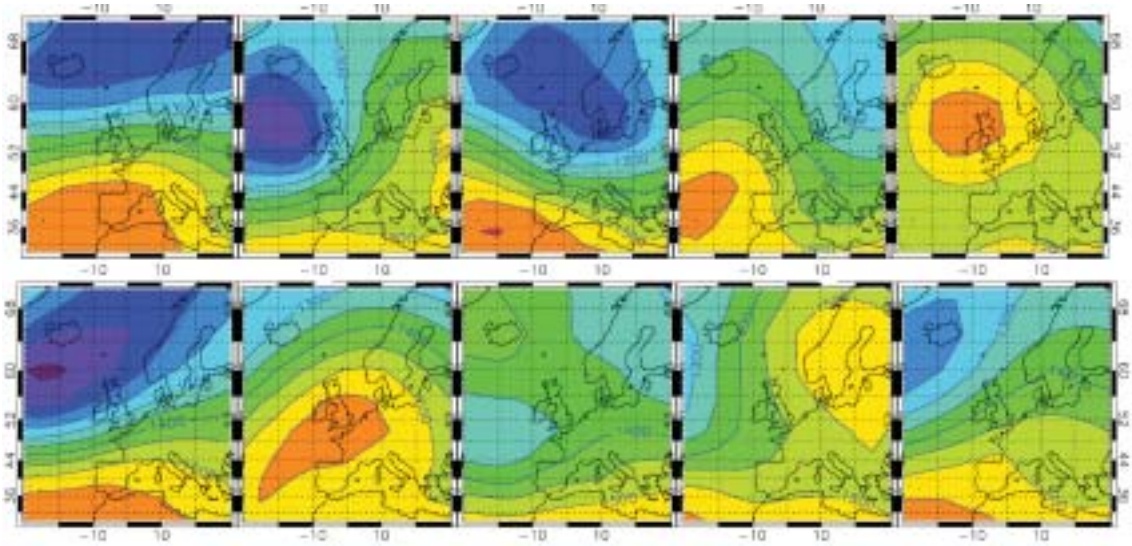

Figure 3.7 Summer 850 hPa pressure surface height (metres) clusters (cluster 1 top left, cluster 2 bottom left, cluster 10 bottom right).

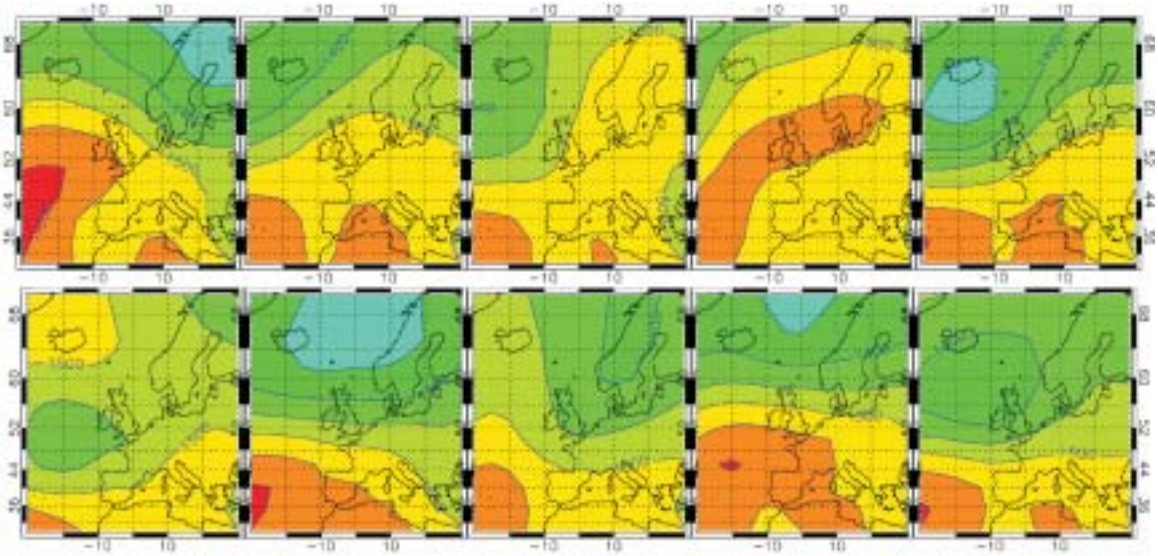

321. Figure 3.6 shows that winter clusters 4 and 9 represent situations where anticyclones (and poor dispersion) dominate UK winter weather most. As the month of lowest incidence of solar radiation (and hence maximum incidence of temperature inversions and poor dispersion) and of minimum vehicle engine efficiency (associated with ambient temperatures), December is especially exposed to conditions of poor dispersion. December 1991, 1992 and 2001 stand out in the recent observational record in terms of the occurrence of consecutive periods of anticyclonic winter clusters 4 and 9. December 1991 and 2001 are also especially prominent in the high NO_2 concentration observational record.

322. The usefulness of this approach is apparent in the analyses of the following high UK NO_2 concentration episodes. The approach also lends itself to an analysis over an extended historical period and can also be applied to climate model output.

3.2.5.2 11th-15th December 1991 – London and South-East England

323. Bower *et al.* (1994) and Derwent *et al.* (1995) provide a detailed analysis of the meteorological conditions which accompanied this noteworthy NO_2 episode. Figure 3.8 presents a timeseries of the NO_2 concentration during this episode.

Figure 3.8 NO_2 concentrations in London 11th–15th December 1991 (µg m^{-3}).

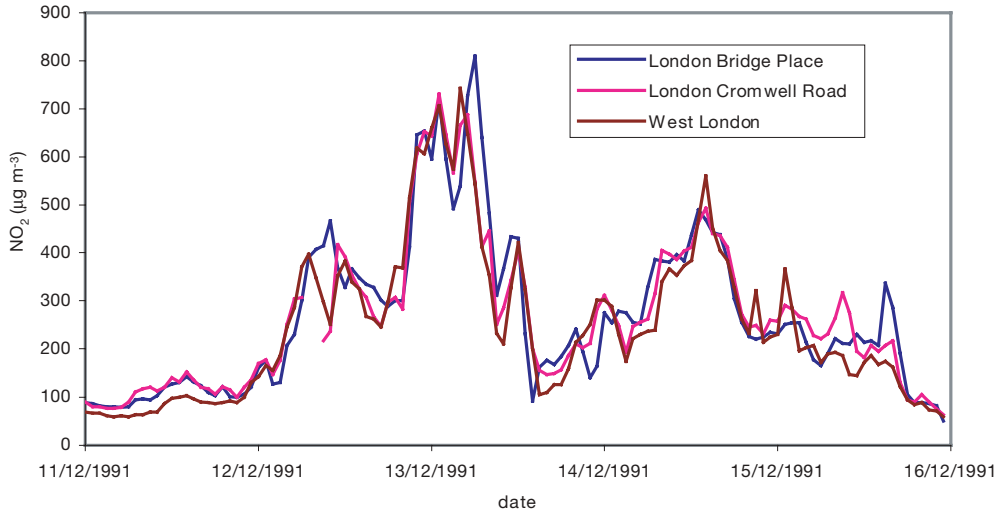

324. The period 2nd-6th December 1991 was classified as being of Winter cluster type 9, followed by a spell of cluster 4 over the period 7th-16th December (Figure 3.6). This was an extended period of light winds, low insolation levels (exacerbated by periods of fog), temperature inversions and poor dispersion generally.

325. Figure 3.9 presents a composite sea-level pressure chart for the duration of the main period of the episode, 12th-15th December 1991, demonstrating the relatively weak pressure gradients and the influence of an anticyclone centred over the near continent.

Figure 3.9 Composite sea-level pressure analysis for the period 12th-15th December 1991.

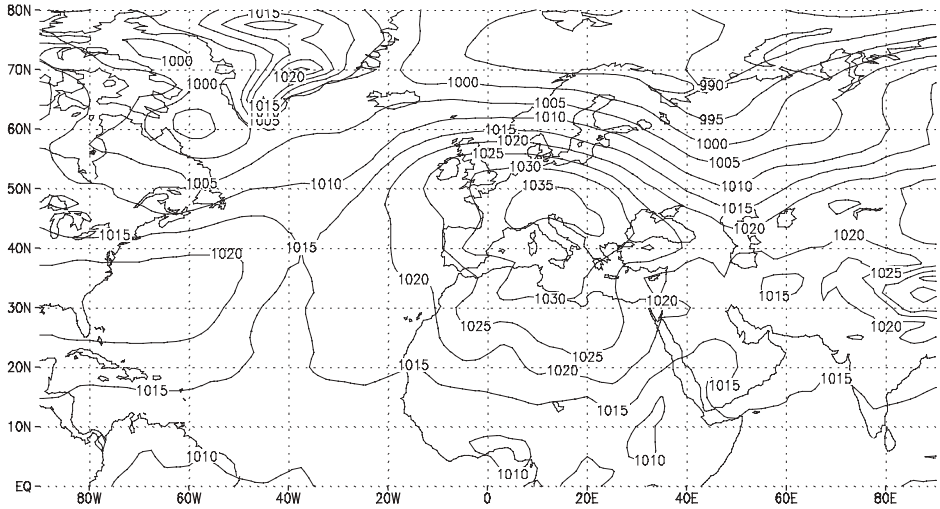

3.2.5.3 11th-12th December 2001 – North-West Britain

326. A timeseries of NO_2 concentrations during this episode is presented in Chapter 6. Figure 3.10 presents the sea-level pressure analysis for the 12th December 2001 by way of example. On this occasion an example of winter cluster 4 occurred between 4th and 8th December,

followed by consecutive examples of cluster 9 between the 9th and the 18th (Figure 3.6). This sequence was the reverse of the conditions accompanying the December 1991 episode considered previously, and led to cities in NW Britain (Glasgow, Manchester, Belfast) being more severely affected this time. However, once again, an extended period of relatively calm weather was shown to be necessary.

Figure 3.10 Sea-level pressure analysis for 00z 12th December 2001.

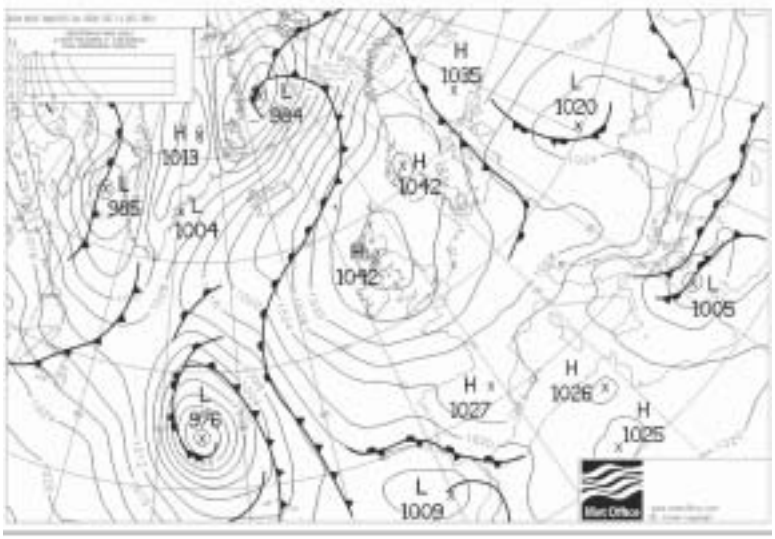

3.2.5.4 26th June 2001 – London and the South-East of England

327. A timeseries of NO_2 concentrations during this episode is presented in Chapter 6. Maximum temperatures on this day rose to 30°C and the sea-level pressure analysis chart is shown in Figure 3.11.

Figure 3.11 Sea-level pressure analysis for 00z 26th June 2001.

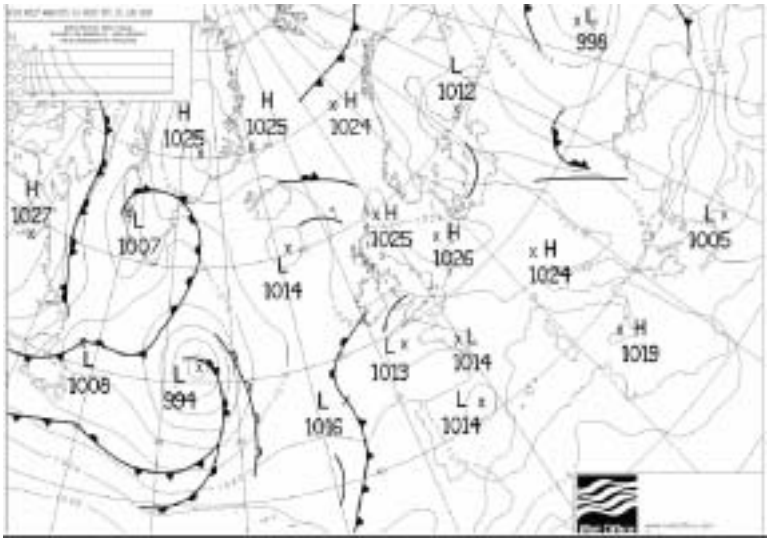

328. Summer Cluster 6 (Figure 3.7) best represents the situation where a ridge of high pressure over Western Europe is leading to advection over Southern Britain from the European continent. It is not surprising that this cluster was indeed found to best describe conditions over the period 17th-26th June 2001.

329. High concentrations of European-derived O_3 are likely to have been available to promote NO_2 formation in polluted environments, especially in SE England. Jenkin *et al.* (2002) have shown that there is a tendency in the UK for O_3 episodes to preferentially occur later in the working week as a result of the accumulation of precursor pollutants and the timescales involved in their advection from source regions.

3.2.5.5 Trends

(a) Historical

330. Middleton and Dixon (2001) show that a significant declining frequency of 'calm' conditions appears to be evident in the station wind data collected at Heathrow Airport over the period 1949-1997. This same trend is also evident when considering December alone, although December 1991 stands out as a very high frequency 'calm' month, in keeping with the episode discussion above.

331. A regional scale quantification of poor dispersion conditions can be derived through the use of a stagnation index. After analysing the meteorological characteristics of recent historical NO_2 episodes, Dorling *et al.* (2003) defined a stagnation index over the UK where the criteria for stagnation are the persistence for three days or more of:

- a high pressure feature over the UK and/or immediate surroundings with central pressure greater than 1030 hPa;
- a sea-level pressure gradient over the UK of < 2.5hPa/250km (equivalent to a surface windspeed of <3.2 m s^{-1}).

332. Application of these criteria to the 2.5°x2.5° resolution NCEP re-analysis dataset (Kalnay *et al.,* 1996) over the period 1960-2001 generates the stagnation frequency results for the month of December shown in Figure 3.12. The episodes in December 1991 and 2001 discussed in sections 3.2.5.2 and 3.2.5.3 clearly affect the frequency data shown. Also interesting, however, is the significant interannual variability and relatively low frequency of stagnation events in the 1960's.

Figure 3.12 December Stagnation Day frequency over the UK derived from the NCEP re-analysis dataset.

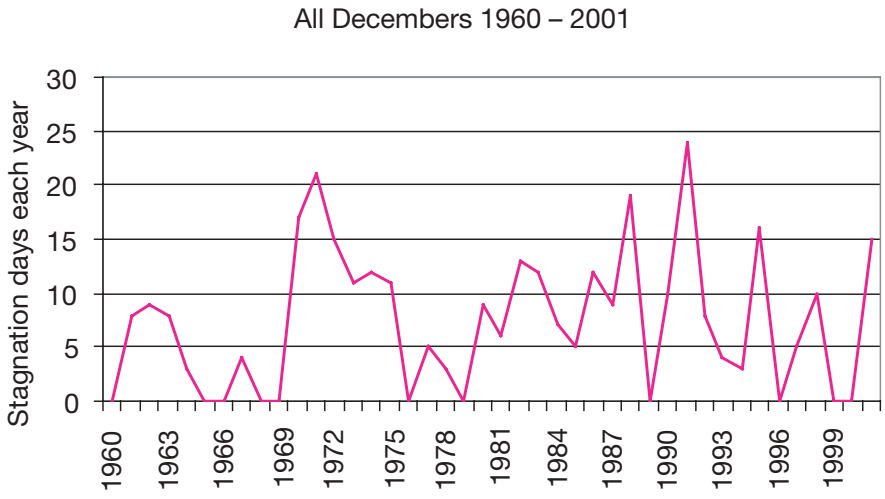

(b) Future

333. The stagnation index definition described above can also be applied to the output of the UK Meteorological Office 50 km resolution Regional Climate Model, HadRM3 (Dorling *et al.*, 2003). The HadRM3 control climate (1960-90) simulation of the seasonal cycle of stagnation frequency over the UK is very similar to that observed in the NCEP re-analysis dataset. This result encourages consideration of the HadRM3 simulation of stagnation frequency in the future climate period, 2070-2100. Table 3.2 presents the stagnation frequencies simulated in the winter months in the HadRM3 control climate (H3B2a_achgi) and in two 2070-2100 climate change scenarios (Hulme *et al.*, 2002) known as 'Mitigation' (Medium-Low H3B2a_ackdd) and 'Business as Usual' (Medium-High H3A2a_ackda).

Table 3.2 Percentage Frequency of Total Stagnation Days for the HadRM3 Control Climate (achgi) and the 'Mitigation' (ackdd) and 'Business as Usual' (ackda) 2070-2100 simulations.

% Days	Dec	Jan	Feb	Winter	Year
1960-1990 Control Climate	10.97	14.62	15.48	13.69	9.43
2070-2100 Business as Usual	7.74	5.48	8.06	7.10	6.31
2070-2100 Mitigation	11.29	7.96	12.04	10.43	7.81

334. Taking the winter as a whole, both of the future scenarios show a substantial fall in stagnation day frequency over the UK relative to the control climate period. However, the 'Business as Usual' emission scenario leads to the more dramatic frequency reduction of almost 50%. These findings are consistent with the more general trends in winter windspeeds reported in Hulme *et al.* (2002) and Anderson *et al.* (2000).

3.3. Chemical processes

335. NO_2 is predominantly a secondary pollutant, its major atmospheric source being the oxidation of emitted NO. An understanding of the chemical processes which produce and destroy NO_2 is therefore central to interpretation of ambient measurements, and to the prediction of how its concentration is likely to vary with implementation of NO_x emissions controls. In this section, a description of the main chemical and photochemical reactions which influence the level of NO_2 is provided.

336. In this section (and in section 5.2.4), graphs which present data for either O_3 or oxidant (defined below), in addition to NO_2, exceptionally make use of ppb units in preference to µg m^{-3}. This is because the ideas and relationships which are being presented relate directly to the chemical coupling of NO, NO_2 and O_3, as described by reactions (1) – (3). The reactions occur on a molecular basis, such that one molecule (or ppb) of NO in reaction (1) reacts with one molecule (or ppb) of O_3, to generate one molecule (or ppb) of NO_2 (in mass terms 1 µg m^{-3} NO reacts with 1.60 µg m^{-3} O_3 to generate 1.53 µg m^{-3} NO_2). It is therefore more logical and instructive to present the data in the molecular units in these instances.

3.3.1. Interconversion of NO and NO_2

337. Under the majority of atmospheric conditions, the dominant pathway by which NO is converted to NO_2 is via the reaction with O_3 (see Figure 3.13):

$$NO + O_3 \rightarrow NO_2 + O_2 \qquad (1)$$

338. At polluted locations comparatively close to sources of NO_x, NO is in large excess and the availability of O_3 provides a limit to the quantity of NO_2 that can be produced by this reaction. The timescale for consumption of O_3 depends on the concentration of NO. At the high end of the range of hourly-averaged concentrations generally observed at polluted roadside locations (ca. 1 ppm), the time constant for O_3 consumption is ca. 2 seconds, with this lifetime increasing at lower levels of NO, in inverse proportion. At unpolluted locations, when O_3 is present in excess, the timescale for conversion of NO to NO_2 by reaction (1) is ca. 90 seconds, at a typical boundary layer background concentration of 30 ppb O_3. At intermediate levels of NO_x, when neither NO nor O_3 is in large excess, reaction (1) progressively depletes both reagents, and the reaction time constant can become very long. For example, in an airmass initially containing 15 ppb of both NO and O_3, it takes ca. 30 minutes for 90% conversion of NO (or O_3) to NO_2 by reaction (1).

Figure 3.13 Schematic representation of the main pathways interconverting NO and NO_2 in the atmosphere. Sources of free radicals which promote the free radical catalysed VOC oxidation (and NO-to-NO_2 conversion) are discussed in the text.

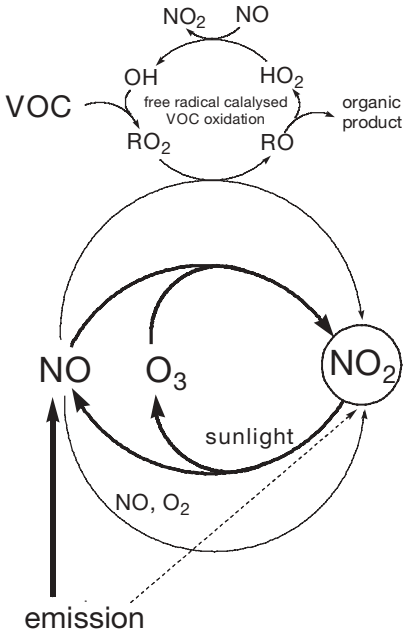

339. During daylight hours, NO_2 is converted back to NO as a result of photolysis, which also leads to the regeneration of O_3 as follows,

$$NO_2 + \text{sunlight} \rightarrow NO + O \qquad (2)$$

$$O + O_2 (+M) \rightarrow O_3 (+M) \qquad (3)$$

where M is a third body, most commonly N_2. As a result of this efficient interconversion by reactions (1) – (3), the behaviour of NO and NO_2 is highly coupled under atmospheric conditions, and it is convenient to refer to these species collectively as NO_x. Because this coupling also involves O_3, however, NO_2 and O_3 are also often collectively defined as 'oxidant (OX)'. Consequently, reactions (1) – (3) are a cycle with no net chemistry, which has the overall effect of partitioning NO_x between its component forms of NO and NO_2, and OX between its component forms of O_3 and NO_2, but leaving the total concentration of both NO_x and OX unchanged.

340. The lifetime of NO_2 with respect to photolysis in the boundary layer depends on latitude, season and time of day. As shown in PORG (1997), summertime measurements indicate that the minimum lifetime of NO_2 under conditions typical of the UK is of the order of 100 seconds, with a mean daylight lifetime of ca. 3 minutes. In the wintertime, this is typically a factor of two or three longer. Under conditions when photolysis is sufficiently rapid, NO, NO_2 and O_3 are potentially in chemical equilibrium, a condition usually referred to as 'photostationary state' (Leighton, 1961). The above cycle predicts that the photostationary state concentrations of the three species are related by the expression $[NO].[O_3]/[NO_2] = J_2/k_1$, where J_2 is the rate coefficient of NO_2 photolysis, and k_1 is the rate coefficient for the reaction of NO with O_3.

341. For a variety of reasons, this relationship does not always hold precisely (for example, see Calvert and Stockwell, 1983; Carpenter *et al.*, 1998). As shown in Figure 3.14a, however, it does provide a good semi-quantitative description of how daylight ambient concentrations of NO, NO_2 and O_3 vary with concentration of NO_x, consistent with the chemical coupling of these species being dominated by reactions (1) – (3). These data indicate that the NO_x crossover point (i.e., when $[NO] = [NO_2]$) typically occurs at about 115 µg m^{-3} NO_x, as NO_2 (60 ppb NO_x). At lower levels, NO_2 is the major component of NO_x, whereas NO dominates at higher concentrations. The OX crossover point (i.e., when $[O_3] = [NO_2]$) typically occurs at about 25 ppb NO_x, with O_3 being the dominant form at lower levels, and NO_2 dominating at higher levels. This pattern is typical, although the precise crossover points vary with conditions (for example, with the value of J_2).

342. Figure 3.14a thus clearly shows how the decrease in O_3 concentration as NO_x increases, is accompanied by an approximately corresponding increase in NO_2 concentration. It also shows, however, that NO_2 levels continue to increase with NO_x even when O_3 levels are close to zero (i.e. at > ca. 100 ppb NO_x). Indeed, Figure 3.14b shows that total OX appears to increase approximately linearly with NO_x over the entire range, such that the level of OX at a given location has a NO_x-independent contribution, and a NO_x-dependent contribution. The former is effectively a 'regional' contribution which equates to the regional background O_3 level, whereas the latter is effectively a 'local' contribution which correlates with the level of primary pollution. Elevated levels of OX at urban locations (i.e. mainly NO_2) may therefore be generated either by having a large local source of oxidant (i.e. high NO_x levels), or by having a large regional source of oxidant in the presence of moderate NO_x levels. The former conditions are most likely to occur in wintertime episodes, when levels of NO_x ca. 700 ppb are typically required for the hourly threshold of 105 ppb (200 µg m^{-3}) to be exceeded for NO_2. During summertime, when boundary layer depths are much greater, such levels of NO_x are less common and NO_2 exceedences are only likely to occur when there is a large regional input of oxidant resulting from elevated background O_3 levels during photochemical pollution episodes (for example, as described by Jenkin *et al.*, 2002).

Figure 3.14 Example of variation of daylight average concentrations of (a) O_3, NO and NO_2, and (b) oxidant (OX = O_3 + NO_2) with level of NO_x. Data are presented for each day of November 1998 and 1999 at Marylebone Rd., Bloomsbury, Hillingdon, Teddington, Reading and Harwell. The lines in (a) were calculated with the assumption of photostationary state, using a daylight-averaged value of $J_2 = 2.9 \times 10^{-3}$ s^{-1}, with OX constrained to values described by [OX] = 31.1 + 0.104.[NO_x], based on a linear regression of the data presented in (b) (adapted from Clapp and Jenkin, 2001).

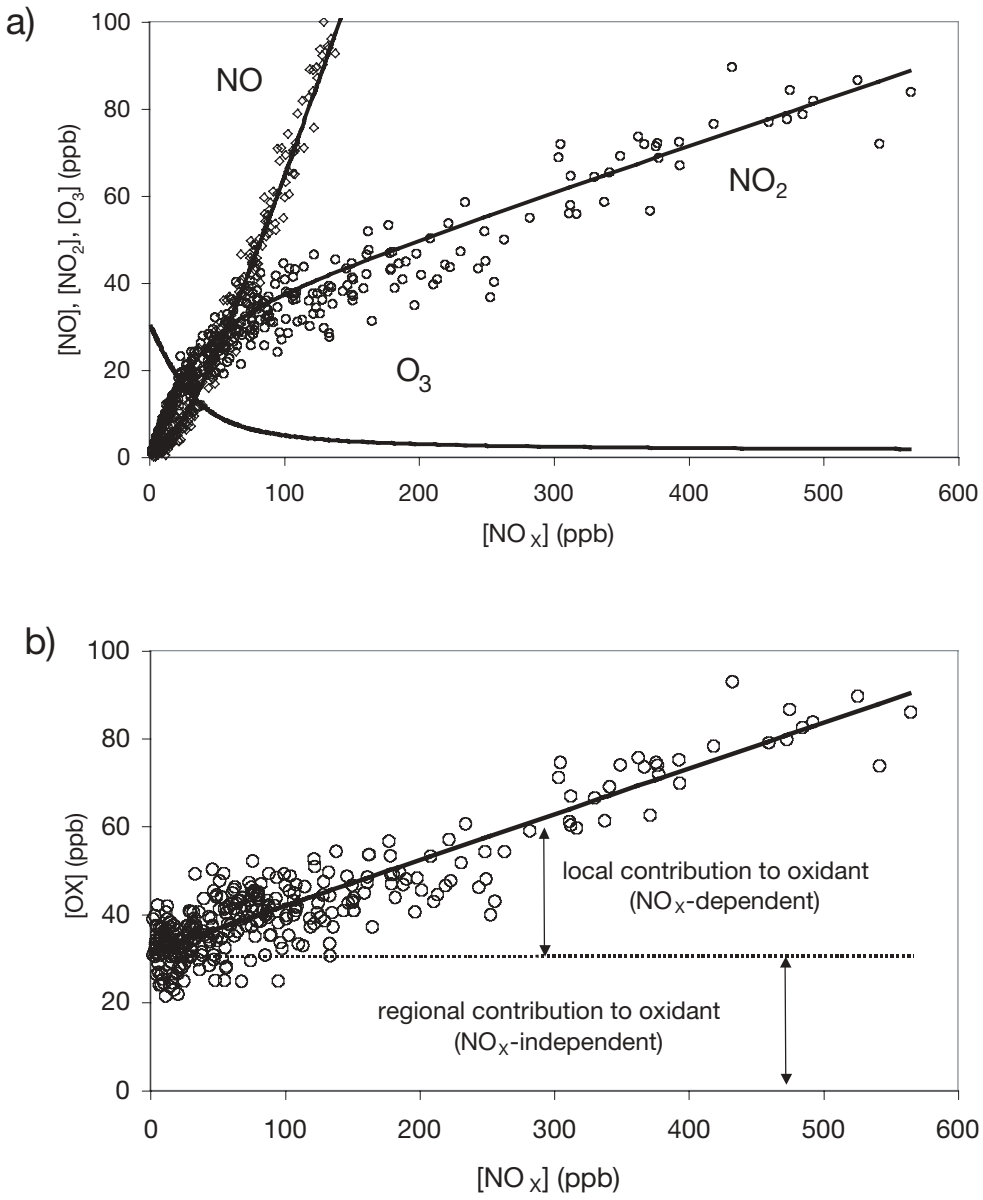

343. A significant proportion of the local contribution is likely to result from primary emission of NO_2, this is variable, but is believed to account for ca. 5% of emitted NO_x, on average. Additional thermal and photochemical sources also potentially contribute, as shown schematically in Figure 3.13. These are all processes which convert NO to NO_2 without associated removal of O_3, and are therefore net sources of OX. Some conversion of NO to NO_2 can potentially occur from the termolecular reaction of NO with O_2:

$$2\ NO + O_2 \rightarrow 2\ NO_2 \qquad (4)$$

344. The rate of this reaction is strongly dependent on the NO concentration, such that it is much more rapid at the elevated levels typical of those close to points of emission. For example, the time for 1% conversion of NO to NO_2 by this reaction is ca. 20 seconds at 100 ppm NO in air, but increases dramatically as NO is diluted. At 1 ppm NO (i.e. the high end of the hourly averaged values observed at roadside locations) the time for 1% conversion is ca. 30 minutes. The extent to which this reaction can contribute is therefore strongly influenced by the rate at which NO is diluted following emission. It is probable that only limited NO to NO_2 conversion by reaction (4) occurs under typical ambient conditions. However, under wintertime pollution episode conditions, when a shallow inversion layer can lead to a combination of high NO_x levels and stagnant air for periods of a day or more (for example, QUARG, 1993; Bower *et al.*, 1994), reaction (4) can potentially make a substantial contribution to OX generation.

345. Other chemical processes which convert NO to NO_2 involve the formation of free radicals, which can catalyse the oxidation of emitted volatile organic compounds, VOC. As shown in Figure 3.13, the reactions of the hydroperoxy radical (HO_2) and organic peroxy radicals (RO_2) with NO,

$$HO_2 + NO \rightarrow OH + NO_2 \qquad (5)$$

$$RO_2 + NO \rightarrow RO + NO_2 \qquad (6)$$

contribute to the catalytic VOC oxidation cycles, and provide the necessary coupling between the VOC and NO_x chemistry. For these cycles to contribute significantly to NO to NO_2 conversion (and therefore OX formation) under urban conditions, significant sources of free radicals (hereafter referred to as 'HOx') are required to initiate the process. A number of thermochemical and photochemical sources of potential significance have been identified, which involve species emitted concurrently with NO_x. The formation of HOx from the thermal reactions of alkenes with O_3 has received particular attention (Paulson and Orlando, 1996; Bey *et al.*, 1997), and these reactions potentially contribute at moderate NO_x levels when O_3 is also available. The thermal reactions of NO_2 with some conjugated dienes emitted from road transport have also been found to generate significant yields of HOx radicals (Atkinson *et al.*, 1984; Shi and Harrison, 1997; Jenkin *et al.*, 2003). These reactions are comparatively slow, however, such that they are only likely to contribute under wintertime pollution episode conditions when boundary layer levels of NO_x and VOC are significantly elevated (Harrison *et al.*, 1998).

346. A detailed discussion of the comparative importance of photochemical sources of HOx radicals for a variety of conditions is available elsewhere (for example, PORG, 1997; Jenkin and Clemitshaw, 2000). Under polluted conditions, the photolysis of formaldehyde, HCHO (and possibly other carbonyls), and nitrous acid, HONO, have been identified as potentially important:

$$HCHO + \text{sunlight } (+2O_2) \rightarrow CO + HO_2 + HO_2 \qquad (7)$$

$$HONO + \text{sunlight} \rightarrow OH + NO \qquad (8)$$

347. Both species are known to be emitted in road traffic exhaust (PORG, 1993), such that their emissions correlate with NO_x. HONO is particularly photolabile, its photolysis lifetime being typically 15 and 40 minutes under daylight-averaged midsummer and midwinter conditions, respectively (PORG, 1997).

3.3.2. Chemical removal of NO_x

348. NO and NO_2 are efficiently interconverted during daylight hours by the processes described above. Other atmospheric chemical transformations of NO_x typically occur on a longer timescale, leading to the generation of a variety of inorganic and organic oxidised nitrogen compounds. Together with NO and NO_2, these species are usually collectively referred to as 'NOY'. The various compounds make variable contributions to NOY, and their formation and removal chemistry is described in detail elsewhere (for example, PORG, 1997; Jenkin and Clemitshaw, 2000). The predominant loss process for NO_x results from its conversion to 'nitrate', either in the form of gaseous nitric acid (HNO_3) or nitrate aerosol, followed by physical removal by dry or wet deposition. The formation of other oxidised nitrogen compounds, such as HONO and peroxyacetyl nitrate (PAN), are only temporary loss processes for NO_x under boundary layer conditions, since these species are broken down comparatively efficiently to regenerate NO_x. However, they potentially have additional significance through interfering with measurement of NO_2 by widely applied techniques. In the present section, attention is therefore given to describing the chemical processes which lead to the formation of nitrate, HONO and PAN in the boundary layer.

3.3.2.1 Formation of nitric acid (HNO_3) and nitrate aerosol

349. The predominant chemical removal route for NO_x during daylight is the reaction of OH with NO_2, which can therefore play a major role in controlling the ambient NO_x concentration:

$$OH + NO_2 (+M) \rightarrow HNO_3 (+M) \qquad (9)$$

350. At a typical background OH concentration of 0.04 ppt, NO_2 is converted to HNO_3 at about 5% hr^{-1} by this reaction, although the conversion rate is correspondingly more rapid at elevated OH concentrations consistent with a photochemical episode (i.e. up to ca. 0.1 ppt). HNO_3 therefore becomes an increasingly important component of NOY downwind of source regions (for example, Harrison *et al.*, 1999). It is removed comparatively efficiently from the troposphere by both wet and dry deposition (for example, Huebert and Robert, 1985; Derwent *et al.*, 1988), and also by adsorption on, or reaction with, the tropospheric aerosol (for example, Cox, 1988; Fenter *et al.*, 1995), leading to the formation of nitrate aerosol. Reaction of HNO_3 with gaseous ammonia also leads to ammonium nitrate aerosol formation, which is a reversible temperature and humidity-dependent process (PORG,1997).

351. Nitrate aerosol is also generated via the formation of the higher oxides, NO_3 and N2O5, as follows:

$$NO_2 + O_3 \rightarrow NO_3 + O_2 \qquad (10)$$

$$NO_3 + NO_2 (+M) \rightleftharpoons N_2O_5 (+M) \qquad (11,-11)$$

$$N_2O_5 + H_2O (+aerosol) \rightarrow 2\ HNO_3 (ads) \qquad (12)$$

352. This reaction sequence is very inefficient during the day, and at higher levels of NO, because NO_3 photolyses and reacts with NO rapidly, leading to NO_x regeneration. During the night, however, conversion of NO_2 to nitrate aerosol by this route potentially occurs on the timescale of a few hours, although the efficiency can be reduced by the reaction of NO_3 with residual NO or with some organic compounds. The latter may either regenerate NO_x, or form a variety of oxidised organic nitrogen compounds or gaseous HNO_3 (for example, Jenkin and Clemitshaw, 2000).

3.3.2.2 Formation of nitrous acid (HONO)

353. In addition to its direct emission from combustion sources, HONO is generated from chemical processing of NO_x During daylight, the reaction of OH with NO leads to the production of HONO:

$$OH + NO\ (+M) \rightarrow HONO\ (+M) \qquad (13)$$

354. At a typical background OH concentration of 0.04 ppt, NO is converted to HONO at about 4% hr^{-1} by this reaction. However, HONO only acts as a temporary reservoir for NO_x during daylight because of its comparatively efficient photolysis (reaction (8)), such that HONO cannot accumulate as a result of reaction (13). Observational data are consistent with the existence of additional thermal sources of HONO, which may operate throughout the diurnal cycle, leading to an accumulation of HONO during the night, followed by photolysis at sunrise (for example, Harris *et al.*, 1982; Kessler and Platt, 1984; Harrison *et al.*, 1996). The precise formation mechanism is unknown, although published information is consistent with HONO production from heterogeneous reactions of NO_2 on land or aerosol surfaces (for example, Lammel and Cape, 1996). Recent studies have demonstrated that diesel exhaust particulates are particularly reactive, and may represent an important substrate for HONO formation (Gutzwiller *et al.*, 2002).

355. Ambient $[HONO]/[NO_x]$ ratios as high as 0.04 have been observed at urban locations (for example, Lammel and Cape, 1996), with contributions to HONO potentially being made by both emissions and secondary reactions of NO_x. Reported measurements of HONO at Marylebone Rd., London (Martinez-Villa *et al.*, 2003) indicated $[HONO]/[NO_x]$ ratios of about 0.01, with the major contribution to the observed HONO being attributed to road transport emissions. As shown in Figure 3.15, $[HONO]/[NO_2]$ therefore tended to increase at higher NO_x (i.e. as $[NO_2]/[NO_x]$ decreased), but typically fell in the range 0.01-0.1 (mean ≈ 0.05). HONO at this level potentially makes a small, but significant contribution to measurements of NO_2 made by chemiluminescent analysers with thermal converters.

Figure 3.15 Observed $[HONO]/[NO_2]$ ratios as a function of NO_x at Marylebone Rd, 11-24th October 1999 (Martinez-Villa *et al.*, 2003). Each data point is based on 15 minute averaged concentrations of HONO and NO_2. Raw data kindly supplied by K. Clemitshaw, Imperial College, London.

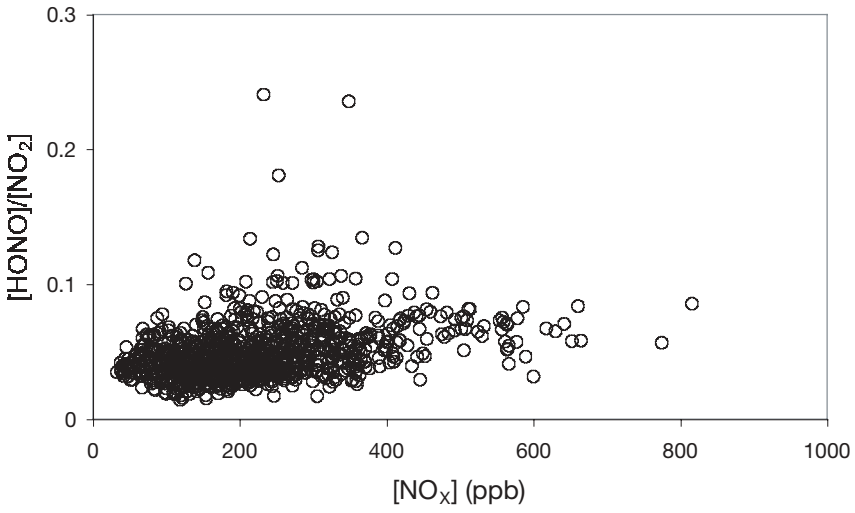

3.3.2.3 Formation of peroxyacetyl nitrate, PAN ($CH_3C(O)O_2NO_2$)

356. The reactions of NO_2 with organic peroxy radicals (RO_2) in general lead to the production of organic peroxy nitrates (RO_2NO_2). The majority of such compounds are thermally very unstable under boundary layer conditions. However, those peroxy radicals containing a carbonyl (C=O) group adjacent to the peroxy radical centre form peroxy nitrates which possess significantly greater stability. The simplest example of this class of compound, peroxy acetyl nitrate or PAN ($CH_3C(O)O_2NO_2$), is thus generated as follows,

$$RC(O)O_2 + NO_2 (+M) \rightleftharpoons RC(O)O_2NO_2 (+M) \qquad (14,-14)$$

where the organic group R is CH_3. Higher homologues are also formed in the atmosphere, but are generally far less abundant than PAN (for example, Altschuller, 1993). This is mainly because the precursor peroxy radical, $CH_3C(O)O_2$, is potentially produced from the degradation of a large number of emitted VOC ≥ C_2, whereas the abundance of potential source compounds systematically diminishes for the larger $RC(O)O_2$ radicals.

357. The ambient concentration of PAN is determined by a balance between its production by reaction (14) and loss by thermal decomposition (the reverse reaction (-14)). Its production rate is highest under conditions when efficient photochemical processing of VOC occurs, because ambient levels of free radicals, including $CH_3C(O)O_2$, are elevated under such conditions. However, the thermal decomposition rate of PAN also tends to be greater under such conditions, because the temperature is higher: the thermal decomposition lifetime of PAN is strongly dependent on temperature, varying from about 1 hour at 298 K to about 2.5 days at 273 K. As a result, historical concentration data measured at rural sites at Harwell (Oxfordshire) and Bush (Midlothian) demonstrate significant levels of PAN throughout the year, with the maximum values (on a weekly-averaged basis) typically occurring in the springtime (PORG, 1993, 1997; Cape and McFadyen, 2001).

358. In addition to the above factors, formation of PAN is also favoured at higher $[NO_2]/[NO]$ ratios which, as shown in Figure 3.14a, are observed at lower NO_x levels. This is because $CH_3C(O)O_2$ also reacts rapidly with NO in competition with reaction (14). This is clearly illustrated in Figure 3.16, which presents data measured in Ascot (Berkshire) in the summer of 1999 (Andres-Hernandez and Burrows, private communication). The observed $[PAN]/[NO_2]$ ratio thus varies from as high as 0.17 at low NO_x (i.e. high $[NO_2]/[NO]$) on a photochemical episode day, to essentially zero at the high end of the NO_x range (i.e. high $[NO]/[NO_2]$) under non-episodic conditions. Over the entire 3-week period of the measurements, the average $[PAN]/[NO_2]$ ratio was ca. 0.02, with the mean $[NO_2]$ ≈16 ppb. PAN therefore potentially makes a small, but significant contribution to measurements of NO_2 made by chemiluminescent analysers with thermal converters, at lower NO_x levels.

Figure 3.16 Observed [PAN]/[NO_2] ratios as a function of NO_x at Silwood Park, Ascot, Berkshire 24th July – 12th August 1999. Each data point is based on 30 minute averaged concentrations of PAN and NO_2. Squares are daylight data on photochemical episode days (defined by mean O_3 > 50 ppb); circles are daylight data on other days; triangles are nighttime data. Data kindly supplied by M. Andres-Hernandez and J. Burrows, IUP, Bremen.

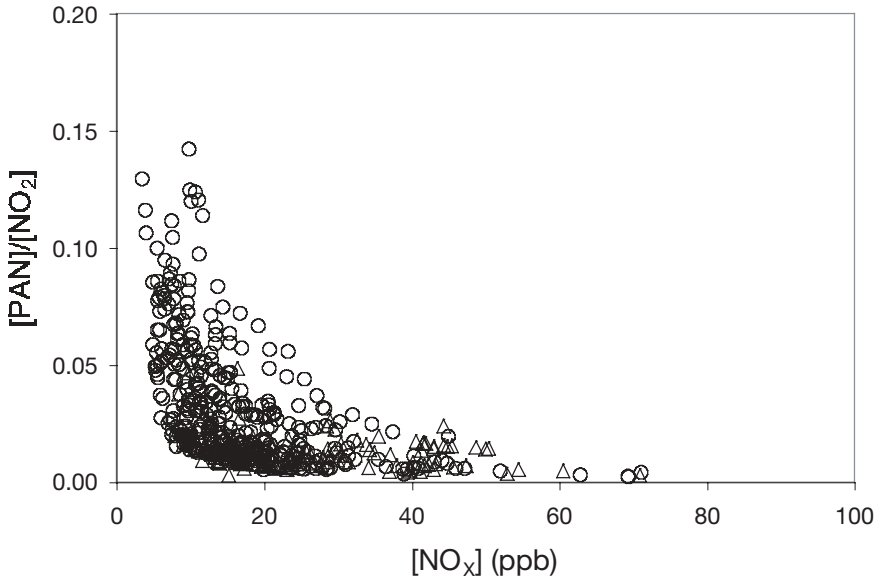

3.3.3 Deposition of NO_2

359. The removal of NO_2 by dry deposition occurs slowly, and represents only a minor loss process. Studies of the rates of deposition onto terrestrial surfaces have generally focused on uptake by vegetation, and have demonstrated that this is dominated by stomatal absorption (for example, Hargreaves *et al.*, 1992). The reported deposition velocities (typically 0.5 – 2 mm s^{-1}) are consistent with NO_2 lifetimes of several days or greater with respect to removal by deposition.

360. As indicated above, NO_2 may also be removed by reaction on non-vegetated land surfaces, with the probable generation of HONO. Reported studies suggest that the reaction may involve adsorbed water, leading to the disproportionation of NO_2 into gaseous HONO and adsorbed HNO_3 (Lammel and Cape, 1996),

$$2\ NO_2(g) + H_2O(ads) \rightleftharpoons HONO(g) + HNO_3(ads) \qquad (15)$$

such that oxidised nitrogen is lost to the ground as HNO_3. Kitto and Harrison (1992) reported evidence for a surface source of HONO by reaction of NO_2, and Harrison *et al.* (1996) derived an effective conversion rate of (5.6 x 10^{-6} x 100/h) s^{-1} (where h is the mixing height in m) in the suburban boundary layer. This suggests a typical lifetime of NO_2 of at least several days with respect to conversion to HONO at the ground. If reaction (15) is an adequate representation of the chemistry occurring, this is accompanied by simultaneous loss of oxidised nitrogen from the air.

3.4. Factors and processes controlling the distribution of NO_2 in the ambient environment

361. The majority of the NO_x emissions by mass enter the atmosphere as NO and are converted there to form NO_2. A small fraction of the NO_x is emitted to the atmosphere as NO_2. At any point in space and time, then, the NO_2 that is present in the atmosphere may have been directly emitted, that is to say primary NO_2, and some may have been formed in the atmosphere, that is to say is secondary NO_2. More often than not it will be a mixture of both primary and secondary NO_2. It is a vital issue for policy whether the origin of the NO_2 is primary or secondary, because source-receptor relationships are dramatically different for primary and secondary pollutants. The different source-receptor relationships influence the different control policy actions that should be taken so that satisfactory NO_2 air quality can be reached efficiently and effectively in the future.

362. In this section some illustrative situations are reviewed where elevated NO_2 concentrations have been observed and describe how atmospheric processes influence the balance between the primary and secondary sources of NO_2. These situations include:

- an isolated major road in a rural environment;
- an isolated major road in an urban environment.

3.4.1. Distribution of NO_2 downwind of an isolated major road in a rural environment

363. Here air is advected from a rural environment across a major double carriageway road carrying heavy traffic that acts as a large source of NO_x, mainly as NO but with a small percentage of its emissions as NO_2. The air is initially assumed to have pollutant levels typical of a relatively unpolluted rural environment, that is to say containing ppb levels of NO and NO_2 and baseline levels of O_3. Since O_3 concentrations generally increase with height above rural surfaces, the air close to the ground may contain O_3 concentrations of typically 30 ppb, whereas aloft, O_3 concentrations may be 40-45 ppb at heights of 100 m or so. Details of an illustrative calculation are given in Box 3.1, with the results presented in Figure 3.17. The scenario represents the case of a very busy dual carriageway under low wind speed conditions.

364. The air that arrives close to the ground at the upwind carriageway encounters immediately the emissions of NO. At the resultant concentrations of several hundred ppb NO, O_3 reacts quickly with a time constant of a few seconds (see section 3.3.1), which corresponds to a spatial scale of up to a few tens of metres under the conditions of this illustration. This reaction:

$$NO + O_3 \rightarrow NO_2 + O_2 \qquad (1)$$

goes to near-completion so that by the time the air close to the surface has crossed the dual carriageway NO_2 formation has largely ceased. At this point, secondary NO_2 concentrations reach a maximum which approaches initial baseline O_3 concentration in the upwind rural environment. Vertical dispersion acts to reduce secondary NO_2 concentrations, which fall off with height and distance downwind from the dual carriageway. Air that crosses the upwind carriageway at some height above the surface encounters the traffic plume slightly later than air close to the surface. The region of maximum secondary NO_2 concentrations is therefore located further downwind with increasing height above the surface.

Box 3.1: NO_x, NO_2 and O_3 pollution concentrations in the vicinity of a major road

A dual carriageway has been modelled using ADMS-Roads. The road has been modelled as two line sources, each 12m wide with a 2m wide central reservation between them, as shown in the following layout:

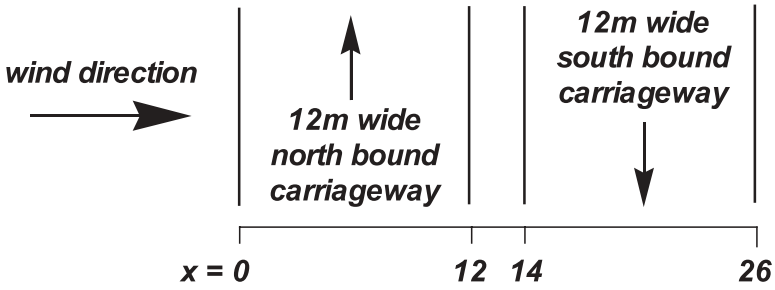

It has been assumed that both sides of the carriageway have equal traffic flows, with 8000 light vehicles per hour driving at 100 km hr^{-1} and 1000 heavy vehicles per hour driving at 90 km hr^{-1}. 1999 DMRB emission factors for the year 2003 have been used to calculate the emission rates on the road, as follows:

Pollutant	Emission per carriageway	Total emission
NO_x (g km^{-1} s^{-1})	4.07	8.13
NO_2 (g km^{-1} s^{-1})	0.41	0.81
VOC (g km^{-1} s^{-1})	0.51	1.02

A background O_3 concentration of 31 ppb has been applied with background NO_x and NO_2 concentrations of 5 ppb and 4 ppb respectively.

Meteorological conditions are as follows: wind speed 2 m s^{-1}, direction of 270 degrees. The modelled hour is 16:00 on May 1st, with a cloud cover of four oktas and a temperature of 15ºC. The resulting boundary layer height is 998 m and the Monin-Obukhov length is -43 m.

Concentrations of NO_x, NO_2 and O_3 have been calculated up to 180 m from the western edge of the road, and up to 25 m in height, as shown in Figure 3.17.

Figure 3.17 Variation of pollutants with distance and height from a 26 m wide road. Concentrations calculated as described in Box 3.1.

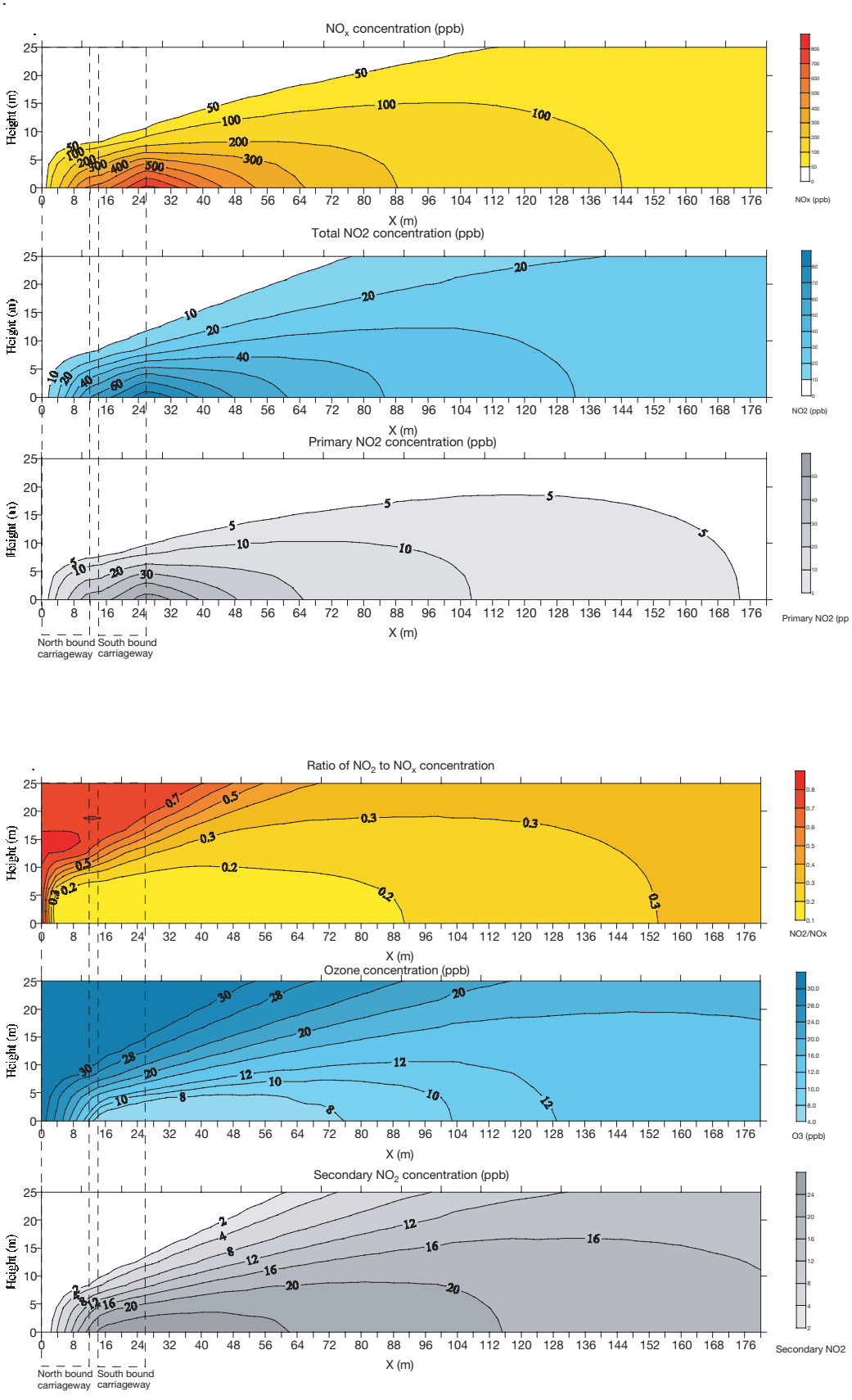

365. Secondary NO_2 concentrations do not fall off as quickly with downwind distance from a major road compared with primary pollutants. This is because NO_2 is still being formed aloft at the top of the traffic plume by reaction between O_3 entrained from the upwind rural environment with NO carried up from the surface by turbulence. This secondary NO_2 is brought down to the surface by turbulent exchange in the downwind environment. Because of the elevated height of this secondary NO_2 source, this downwards turbulent transport has a significantly longer time constant compared with the upwards turbulent transport of the secondary NO_2 formed near the surface. This elevated secondary NO_2 source controls the concentration of secondary NO_2 in the environment downwind of the road edge. However, with increasing downwind distance, secondary NO_2 concentrations eventually begin to fall as vertical exchange depletes the NO concentrations throughout the traffic plume, reducing secondary NO_2 formation.

366. If all the NO_x from traffic was emitted as NO, then the sequence of processes outlined above would entirely control the distribution of NO_2 in the environment downwind of the major road and broadly speaking NO_2 concentrations would never exceed nor even approach the O_3 concentrations in the rural environment upwind of the major road. Direct emissions of NO_2 occur with a small percentage by mass and these generate a distribution of primary NO_2 that is superimposed upon the distribution of secondary NO_2 described above.

367. As air reaches the upwind carriageway, close to the ground, it immediately encounters the direct emissions of NO_2 from the traffic. Primary NO_2 concentrations steadily rise across the upwind carriageway as direct emission competes against vehicle-generated turbulence and vertical dispersion. Somewhere over the downwind carriageway, vertical dispersion starts to dominate over direct emission and primary NO_2 concentrations begin to level off and subsequently start to decrease. At the edge of the downwind carriageway, direct emission of NO_2 ceases and primary NO_2 concentrations fall off steadily with increasing downwind distance. The higher the windspeed, the sooner the primary NO_2 concentration maximum is reached and the lower in magnitude it is. Since traffic emissions have little buoyancy, the concentration contours of this primary NO_2 have their maximum concentrations close to the ground and concentrations fall off rapidly with both height above the surface and downwind distance.

368. If there was no O_3 in the upwind environment, then this direct NO_2 emission together with vertical dispersion and vehicle-generated turbulence would control the distribution of NO_2 downwind of the major road. Inevitably, air parcels arriving at the upwind carriageway of the major road contain O_3 at concentrations close to baseline levels and so account must always be taken of secondary NO_2 formed through the reaction of primary NO with O_3. The distribution of NO_2 downwind of a major road is therefore the sum of the primary and secondary NO_2 distributions and a complex three-dimensional spatial pattern results. The interaction between the processes is illustrated for a two-dimensional section in Figure 3.17.

3.4.2. Distribution of NO_2 downwind of an isolated major road in an urban environment

369. Here air is advected across an urban environment and over a major road carrying heavy traffic that acts as a large source of NO mainly but with a small percentage of its NO_x emissions as NO_2. If the oxidising capacity of the atmosphere has been largely exhausted before the air reaches the upwind carriageway then the air will contain a mixture of NO and NO_2, but O_3 levels may well be a few ppb or less. Under these conditions, little additional secondary NO_2 will be formed close to the road surface and the distribution of NO_2 downwind of the major road will be determined by the primary emissions of NO_2 and the NO_2 distribution upwind of the major road in question.

370. As air reaches the upwind carriageway, NO_2 concentrations will begin to rise as direct emission competes against vertical dispersion and vehicle-generated turbulence. The distribution of primary NO_2 will follow closely that given above for the rural major road under the conditions where no O_3 was present. In the urban case, the distribution of NO_2 downwind of the major road would follow that of any other primary motor vehicle pollutant. NO_2 concentrations would peak close to the kerb of the downwind carriageway and concentrations would fall off rapidly with height and inversely with increasing downwind distance.

371. Secondary NO_2 still continues to be formed aloft in urban areas long after O_3 is depleted close to the surface. At some height, say tens to hundreds of metres above the surface, O_3 will still be present at concentration levels approaching those in the upwind rural environment. NO transported up to this level by turbulent exchange will react with O_3 in a thin layer just below the bottom of the O_3-rich layer. The secondary NO_2 formed here can then be transported down towards the surface by turbulent exchange and mix with the primary NO_2 found close to the surface.

372. During a photochemical O_3 episode, there may be several times more O_3 in the upwind rural environment compared with baseline conditions, for a few hours during mid-afternoon on each of the episode days. This increased O_3 will lead to increased O_3 concentrations within urban areas as NO is converted increasingly to NO_2. Under these conditions, the case of the major road within an urban environment may be changed to look more like the rural case with the overlapping distributions of both primary and secondary NO_2 downwind of the major road.

373. Inevitably in urban areas, the distribution of NO_2 is controlled either by the availability of O_3 from the upwind rural environment or by the availability of NO_x emissions and their split between NO and NO_2. As emission density increases, secondary formation of NO_2 becomes of diminished significance and NO_2 concentrations become increasingly dominated by direct emissions of NO_2. So, for example, the traffic excess of NO_2 found by subtracting the simultaneous NO_2 concentrations observed at the Bloomsbury urban background site from the roadside Marylebone Road site, can be accounted for largely by the direct emissions of NO_2 without any requirement for additional urban conversion of NO to NO_2.